



**Non-radiative deactivation in phenol-pyridine complex:  
Theoretical study**

Journal:	<i>Photochemical &amp; Photobiological Sciences</i>
Manuscript ID:	PP-ART-06-2014-000199.R3
Article Type:	Paper
Date Submitted by the Author:	24-Mar-2015
Complete List of Authors:	Esboui, Mounir; Faculté des Sciences de Tunis, Département de Physique; Institut Supérieur des Sciences et Technologies de l'Environnement Borj Cédria, Département de Physique Chimie Jaidane, Nejmeddine; Faculté des Sciences de Tunis, Département de Physique Tunis, Tunis, Tunisia,

**Non-radiative deactivation in phenol-pyridine complex: Theoretical study**

Mounir Esboui<sup>a,b,\*</sup> and Nejmeddine Jaidane<sup>a</sup>

<sup>a</sup> Laboratoire de Spectroscopie Atomique, Moléculaire et Applications, Département de Physique, Faculté des Sciences de Tunis, 2092 Tunis, Tunisia.

<sup>b</sup> Technical and Vocational Training Corporation, Hail College of Technology, P. O. Box 1960 Hail 81441, Kingdom of Saudi Arabia.

(\*) Corresponding Author : Mounir Esboui

Phone : +966 542427898.

E-mail address: [mounir.esboui@fst.rnu.tn](mailto:mounir.esboui@fst.rnu.tn)

**Abstract**

Minimum energy structures of the ground and lowest excited states of phenol (PhOH)-pyridine (Py) hydrogen bonded complex in the gas phase, were performed by ab initio calculations. Photophysical and photochemical features of the complex under Cs symmetry ( planar (Pl) and perpendicular (Pe) conformers) and without any symmetry constraints (unconstrained (Un) conformer) were studied with respect to the nonradiative decay processes to the ground state. This mechanism involves internal conversion (IC) and intersystem crossing (ISC) along O-H bond elongation coordinate, where the coupled electron/proton transfer reaction plays a decisive role in the photophysics of this complex. For Pl conformer, the nonradiative decay proceeds from a locally excited  $^1\pi\pi^*(LE)$  minimum over a barrier conical intersection (0.12 eV) to a charge transfer (CT) minimum which correspond to a hydrogen bonded  $PhO\cdot\dots HPy\cdot$  bi-radical. Near this latest minimum, a barrierless conical intersection  $^1A'(\pi\pi^*(CT))-S_0$  funnels the electronic population from the CT to the ground  $S_0$  state, completing the nonradiative deactivation. The calculations performed for Pe and Un conformers provided that the same radiationless mechanism proceeds with no  $^1\pi\pi^*(LE)/^1\pi\pi^*(CT)$  conical intersection near the Franck Condon region. Furthermore, the population of the lowest triplet states through ISC and their contribution in the photophysics of PhOH-Py complex have been discussed. These findings seem to suggest that there is not a single dominant path, but rather many distinct paths involving different quenching mechanisms.

**Keywords** : photophysics, photochemistry, conical intersection, charge transfer, excited state deactivation.

## 1. Introduction

Hydrogen bonding has been the subject of contemporary research interest because of its prevalence and importance in various branches of science<sup>1</sup>. It is the most important for structures of the major biological macromolecules, such as proteins and DNA. In particular, excited state hydrogen bonding interaction plays important roles in many photophysical processes and photochemical reactions. Therefore, increasing attention has been paid to the hydrogen bonding dynamics<sup>2,3</sup>. The photostability properties of the hydrogen-bonded complexes have been discussed in many contributions by considering some DNA base pairs,<sup>4,5,6,7,8,9,10,11</sup>. It is commonly believed that ultrafast excited state deactivation via internal conversion to the ground state is the key for the photostability of DNA<sup>12</sup>. For reason of feasible methods for accurate results, simplified aromatic hydrogen-bonded complexes are used as models for the photophysics study of such nonradiative deactivation reactions. At present, there is a good consensus between experimentalists and theoreticians that the ultrafast nonradiative decay of hydrogen-bonded aromatic chromophores is mostly caused by internal conversions through conical intersection between first excited and ground states, which provides an efficient pathway for the depopulation of the lowest singlet excited states<sup>13,14,15,16,17,18,19,20,21,22,23,24,25,26,27</sup>.

In this work, we focus on the photophysics of phenol-pyridine hydrogen-bonded complex, which is a model system wherein both the proton donor and the proton acceptor are  $\pi$  electronic conjugated system. It can also serve as a model for fluorescence quenching through intermolecular hydrogen bonding between aromatic chromophores. Pyridine is well known as an electronic quencher of aromatic molecules. Consequently, this work will be helpful to understand the quenching mechanism of phenol in the excited state by pyridine. Phenol-pyridine (PhOH-Py) complex in the gas phase can adopt numerous low energy structures under Cs symmetry (planar (Pl) and perpendicular (Pe) conformers) and without any symmetry constraints (unconstrained (Un) conformer). As shown in Fig. 1, Pl and Pe conformers differ in the orientation of the pyridine molecule with respect to the plane of phenol ring. For all conformers of PhOH-Py complex, phenol (PhOH) serves as the representative proton donating aromatic chromophore and pyridine (Py) represents an aromatic proton acceptor. For this complex, previous ab-initio MO calculations with the STO-3G minimal basis set show that a slight movement of the proton causes a large amount of charge transfer from proton donor to proton acceptor at the barrier maxima and the energy barrier for proton transfer is relatively low at the  $^1\pi\pi^*$  states of the donor<sup>15</sup>.

The purpose of this work is to explore and compare with computational methods, the photophysics of the PhOH-Py complex in the gas phase under Cs symmetry (Pl and Pe conformers) and without constraints (Un). Thus, we have calculated vertical and adiabatic excitation energies, minimum energy structure of ground and excited singlet and triplet states, as well as potential energy profiles of the reaction paths leading to the nonradiative decay mechanisms taking into account triplet states contribution.

## 2. Computational methods

All calculations were carried out with the TURBOMOLE program package, version 5.8<sup>28</sup>. Ground state structures of PhOH-Py were optimized with Cs symmetry first and then without any symmetry constraints (C1), at the second order Moller-Plesset MP2 level within resolution of the identity (RI) approximation for the electron repulsion integrals (RI-MP2)<sup>29</sup>. For all atoms, the correlation-consistent polarized valence of double- $\xi$  basis set cc-pVDZ quality augmented with diffuse functions aug-cc-pVDZ was used. The use of diffuse basis functions is

required to describe correctly low-lying Rydberg  $\pi\sigma^*$  excited states. The equilibrium geometries of these complexes in the lowest excited singlet and triplet states have been calculated at the second order approximate coupled cluster (CC2) method employing the resolution of the identity (RI) approximation<sup>30,31</sup>, using the aug-cc-pVDZ basis set. For both ground and excited state geometries optimizations, the starting geometries were constructed with Cs and C1 symmetry constraints. Within the Cs point group, The phenol molecule lies in the symmetry plane and the excited state wave functions transform according to A' and A'' irreducible representations. In order to optimize the excited state geometries, the minimum energy structure of the ground state has been chosen as the starting point for lowest excited states. Potential energy (PE) profiles have been calculated along the minimum energy path (MEP) for an elongation of the O-H stretching coordinate in PhOH-Py complex; for a given value of O-H, all remaining coordinates have been optimized.

### 3. Results and discussion

#### 3.1. Ground state equilibrium structures and vertical excitation energies

The ground state  $S_0$  equilibrium geometries of PhOH-Py complex with Cs symmetry (Pl and Pe conformers) and without symmetry constraints (Un conformer) optimized at the RIMP2 level using aug-cc-pVDZ basis set, are shown in Fig 2 (a1), (a2) and (a3). In all conformers, there is a strong hydrogen bond between the OH of phenol with the nitrogen atom of pyridine in this complex, the hydrogen bond CO-H...N remains in the plane of phenol. The minimum unconstrained geometry (Fig 2 (a3)) is almost identical with Pe conformer (Fig 2 (a2)), with the same energy stability. For this we adopt in the following Pe conformer as a representative of unconstrained geometry of the complex. The change of PhOH-Py complex from planar to perpendicular alters the hydrogen bond by more than 0.01 Å, in favor of Pe conformer. Therefore, RIMP2/aug-cc-pVDZ calculation shows that the length of the hydrogen bond between H and N atom is 1.801 and 1.788 Å for the hydrogen-bonded Pl and Pe complexes, respectively, and O-N distance of 2.778 and 2.779 Å. In addition, the hydrogen bond angle of the Pe form is very close to the 180°. This indicates that the hydrogen bond is stronger for the Pe conformer than the Pl one. Thus, for the PhOH-Py complex in the ground state, Pe conformer is calculated to be more stable than Pl, this stability is about 0.02 eV (the binding energy of the intermolecular hydrogen bond O-H...N in Pe and Pl conformers are 0.57 and 0.55 eV, respectively) at the RI-MP2 level (the same stability when the ZPE is taken into account). All optimized structures were confirmed to be minima on the ground state surface by normal mode analysis.

The vertical excitation energies with corresponding transitions, dipole moments and oscillator strengths of the Pl and Pe conformers of PhOH-Py complex were calculated. Table 1 shows these specifications for the lowest three singlet excited states in both A' and A'' symmetries. At the RIC2/aug-cc-pVDZ level of theory, our calculation shows that the lowest  $^1A'$  state has the  $^1\pi\pi^*$  nature for Pl and Pe conformers and exhibits excitation energies in UV range: 4.74 and 4.73 eV, respectively. The lowest  $^1A''$  state has the  $^1\pi\sigma^*$  character for Pl conformer and the  $^1\pi\pi^*$  nature for Pe conformer. These states exhibit an energy higher than the lowest  $^1A'(\pi\pi^*)$  by more than 0.3 eV.

As it can be seen from Table 1, for both Pl and Pe conformers, the calculation of the vertical excitation energy shows that the lowest excited singlet  $S_1$  state,  $^1\pi\pi^*$  originates predominantly from the excitation of an electron from the highest occupied MO (HOMO) of A' symmetry to the (LUMO+14) MO. In this case, both  $\pi$

and  $\pi^*$  orbitals are completely localized on phenol; this state is of a locally excited (LE) character. This  $^1\pi\pi^*(LE)$  is a bright state, which has the largest oscillator strength (more than 0.03) for a transition from the  $S_0$  state. Furthermore, from Table 1, one can find that there are no significant changes of dipole moments between ground and the LE states for both PI and Pe hydrogen bonded complexes. This means that no marked charge redistribution occurs between phenol and pyridine, and this consistent with the LE character of the first excited state. This state is followed by  $^1\pi\pi^*(Py)$  (both  $\pi$  and  $\pi^*$  MO are located on pyridine molecule),  $^1\pi\pi^*(CT)$  ( $\pi$  is located on PhOH and  $\pi^*$  is located on Py),  $^1n\sigma^*$  and  $^1\pi\sigma^*$  excited states in both conformers of PhOH-Py complex. The first lowest excited singlet state of the PI and Pe conformers in  $A''$  symmetry are of a  $^1\pi\sigma^*$  and  $^1\pi\pi^*(CT)$  characters, respectively.

The vertical energy difference between the lowest  $^1\pi\pi^*(LE)$  excited state of  $A'$  symmetry and the lowest CT state is higher for PI conformer by about 0.23 eV than the corresponding value in Pe form. Indeed, the excitation energy of the  $^1\pi\pi^*(LE)$  state remains almost unchanged when passing from PI to Pe conformer, while the position of the lowest CT state is shifted to significantly lower energy. This indicates that the  $^1\pi\pi^*(CT)$  excited state of Pe conformer can be populated from direct excitation energy threshold lower by about 0.23 eV compared to the PI conformer. As seen also in Table 1, the PI and Pe conformers have the same lowest  $^1\pi\sigma^*$  excitation energy (5.17 eV). This can be explained by the character of  $\sigma^*$  orbital associated with the O-H bond, which is independently to the pyridine orientation towards phenol.

The vertical lowest excited state for the isolated phenol in Cs symmetry computed at RICC2/aug-cc-pVDZ, is of  $^1A'(\pi\pi^*)$  character is calculated to lie 4.86 eV above the ground state minimum. The second excited state  $^1\pi\sigma^*$  is located at 5.37 eV. These values are in the range of values reported in previous studies at different levels of theory<sup>32,33,34,35,36</sup>. The interaction of PhOH with Py in both conformers, lowers the energies of the lowest  $^1A'(\pi\pi^*)$  and  $^1\pi\sigma^*$  states by about 0.12 eV and 0.2 eV, respectively.

Previous ab-initio calculations of excitation energies for the phenol dimer show that the two lowest singlet states are of  $^1\pi\pi^*$  character (4.85 and 5.0 eV), followed by two  $^1\pi\sigma^*$  states (5.77 and 5.85 eV)<sup>32</sup>. These results are qualitatively comparable with our present RICC2/aug-cc-pVDZ calculations concerning PI conformer of PhOH-Py complex.

### 3.2. excited state minimum geometries and adiabatic excitation energies

Starting from ground state minimum geometries, the excited state geometries of  $A'$  and  $A''$  symmetries in keeping Cs symmetry as well as the unconstrained geometry have been optimized by the use of RICC2 level with same basis. Fig 2 shows a minimum structure comparison between ground and first excited state PI conformer. For this conformer, the minimum geometry (Fig 2(b1)) of the lowest excited singlet state is of  $^1\pi\pi^*(LE)$  character. Furthermore, upon photoexcitation of this conformer, we note that H...O and O...N distances decrease by 0.16 and 0.13 Å, respectively, while O-H distance in PI increases by 0.04 Å (Fig 2. (a1) and (b1)). As a consequence, the binding energy of the intermolecular hydrogen bond O-H...N between the phenol and pyridine is greatly increased, from 0.55 to 0.69 eV, upon photoexcitation, which facilitates the transfer of proton to pyridine. For Pe and PI conformers, although we attempted to optimize the minimum energy for the  $^1\pi\pi^*(LE)$  state, this RICC2/aug-cc-pVDZ optimization led directly to the coupled electron proton

transferred complex ( $^1\pi\pi^*(CT)$  minimum). Thus for these conformers, the  $^1\pi\pi^*(LE)$  state not exhibits a local minimum.

The adiabatic excitation energies and corresponding transition, dipole moment and oscillator strength of the three lowest excited singlet state at  $A'$  and  $A''$  symmetries of the PI conformer of PhOH-Py complex optimized by RICC2/aug-cc-pVDZ calculation, are given in Table 2. The lowest excited singlet state is of  $^1\pi\pi^*$  character, where  $\pi$  and  $\pi^*$  orbitals are completely localized on Phenol. This  $^1\pi\pi^*(LE)$  state, with its largest oscillator strength (about 0.045), is stabilized by about 0.21 eV relative to the corresponding vertical excitation energies. The adiabatic excitation energy of  $^1\pi\pi^*(LE)$  state of PhOH-Py complex is red-shifted in comparison to the energy of the lowest  $^1\pi\pi^*$  transition of isolated PhOH. RICC2/aug-cc-pVDZ calculation predicts that this shift is of about 0.14 eV (from 4.67 to 4.53 eV). The second lowest excited singlet state is a  $^1\pi\pi^*$  transition of charge transfer (CT) character ( $\pi$  and  $\pi^*$  orbitals are completely localized on phenol and pyridine, respectively) characterized by its large dipole moment (more than 16 D), which is nearly three times larger with respect to the  $^1\pi\pi^*(LE)$  state. For PI conformer, the calculated vertical energy of the  $^1\pi\pi^*(CT)$  excited state is about 0.36 eV higher than the energy of the lowest  $^1\pi\pi^*(LE)$  minimum.

For optimized structure at  $A'$  symmetry, the vertical excitation energies, dipole moment and oscillator strengths of the 3 lowest transitions of  $A''$  symmetry in the PI conformer of PhOH-Py complex were calculated with aug-cc-pVDZ basis set. As it is shown in Table 2, the lowest energy transition of the PI form in  $A''$  symmetry, is of  $^1\pi\sigma^*$  character, this latest is calculated to be the third state after  $^1\pi\pi^*(LE)$  and  $^1\pi\pi^*(CT)$  states, locates at 0.55 eV above the first one.

To depict the nature of the low-lying electronically excited states, the frontier molecular orbitals of both PI and Pe conformers are shown in Fig 3. Herein, we only show the orbitals that contribute to the photophysics of each conformer. According to RICC2 calculations, in both conformer, the first  $A'$  ( $^1\pi\pi^*(LE)$ ) state is dominated by the same excitation from HOMO to LUMO+14. While, the first  $A'$  ( $^1\pi\pi^*(CT)$ ) state mainly corresponds to the LUMO+6  $\leftarrow$  HOMO and LUMO+4  $\leftarrow$  HOMO transitions, respectively in PI and Pe conformer. Also, the first  $A''$  state in Pe conformer, which is of  $^1\pi\pi^*(CT)$  nature, is mostly corresponding to the LUMO  $\leftarrow$  HOMO transition.

The possibility of non-radiative triplet state quenching is still a challenge in the study of photophysical process in PhOH-Py complex. The equilibrium geometries of the triplet electronic states were optimized at RICC2/aug-cc-pVDZ level. The choice to appear triplet states in the study of the excited state photophysics of PhOH-Py complex is that they have attracted strong interest in recent years especially of their population from the lowest singlet excited states<sup>37,38,39</sup>. It is important in this way to know the regions in the excited state relaxation path where the singlet state remains for a longer period of time which allow to the intersystem crossing because singlet-triplet transitions are much slower (few nanosecond).

Table 3 summarizes the computed spectroscopic proprieties of triplet excited states at  $A'$  symmetry in both PI and Pe conformer. It displays the 3 lowest transitions and dipole moment by the use of aug-cc-pVDZ basis set. The calculated adiabatic excitation energies of the lowest triplet excited state are of  $^3\pi\pi^*(LE)$  character for both Pe and PI conformer. The second lowest excited state is a  $^3\pi\pi^*$  transition of charge transfer (CT)

character. For these optimized structures at A' symmetry, the vertical excitation energies and dipole moment of the 3 lowest transitions of A'' symmetry in the Pl and Pe conformers were calculated. As it is shown in Table 3, the lowest excited state transition of the Pl form, is of  $^3A''(\pi\sigma^*)$  character for RICC2/aug-cc-pVDZ. While for Pe conformer, the lowest triplet excited state is of  $^3A''(\pi\pi^*(CT))$  character.

### 3.3. Excited state deactivation pathways

In this section, potential energy profiles of the lowest excited states of Pl, Pe and Un conformers connecting the points having minimum energies are studied with respect to the nonradiative decay process to the ground state  $S_0$ .

#### 3.3.1. Pl conformer

The RICC2/aug-cc-pVDZ calculation is performed to follow the electron/proton transfer reaction between phenol and pyridine in the Pl conformer of PhOH-Py complex. Potential energy (PE) profiles as shown in Fig 4 and Fig 5 have been calculated along the minimum energy path (MEP) for an elongation of the O-H stretching coordinate in the Pl conformer of PhOH-Py complex at both A' and A'' symmetries (in the Cs point group), for a given value of O-H, all remaining coordinates have been optimized for the lowest  $S_1$  excited state. Fig 4 shows the PE profiles of Pl conformer in A' symmetry. The geometries of the lowest ( $^1\pi\pi^*(LE)$  or  $^1\pi\pi^*(CT)$ ), singlet states have been optimized along the reaction path, while the energies of the electronic ground  $S_0$  and triplet ( $^3\pi\pi^*(LE)$  and  $^3\pi\pi^*(CT)$ ) states were calculated along the reaction path optimized in the ( $^1\pi\pi^*(LE)$  or  $^1\pi\pi^*(CT)$ ) state. As it is shown in Fig 4, the upper-lying  $^1\pi\pi^*(CT)$  potential energy profile is strongly repulsive for small O-H distance to attend after a shallow minimum for O-H distance around 2.44 Å. This minimum corresponds to an electron/proton transferred complex (the proton follows the electron) in which the proton has been transferred to pyridine corresponding to a  $^1\pi\pi^*(CT)$  minimum (Fig. 6(a1)), with an energy of about 2.37 eV above the ground state minimum, and lower by about 2.16 eV than the  $^1\pi\pi^*(LE)$  minimum. The low oscillator strengths of the CT state seem to make direct optical access to them from the ground state very improbable. However, the pronounced stabilization of this state is mediated by the re-neutralization of this electronic charge transfer by the transfer of the proton from phenol to pyridine. Whereas, the energies of  $^1\pi\pi^*(LE)$  and  $S_0$  states increase along the O-H reaction coordinate, which are strongly destabilized by the proton transfer facilitating the CT deactivation. As a result, in the Pl conformer of PhOH-Py complex at  $^1\pi\pi^*(LE)$ , two conical intersections are consecutively encountered along the reaction path. The first crossing is about 0.12 eV higher than the  $^1\pi\pi^*(LE)$  minimum, this energy value corresponds also to the energy barrier for the transition from the  $^1\pi\pi^*(LE)$  state to the  $^1\pi\pi^*(CT)$  state. Thus, the lifetime of the  $^1\pi\pi^*(LE)$ , which is controlled by the first crossing (barrier height) should be long. The second crossing of the  $^1\pi\pi^*(CT)$  excited state is with the ground state  $S_0$  at an O-H distance about 2.13 Å is barrierless, which triggers an ultrafast internal conversion process. The energy of this crossing is closer than the energy of the  $^1\pi\pi^*(CT)$  minimum of the electron/proton transferred complex  $PhO\cdots HPy$ . It is worth noting that the barrier energy of the  $^1\pi\pi^*(LE)$ - $^1\pi\pi^*(CT)$  conical intersection shown in Fig 4 is lower than the vertical excitation energy of the  $^1\pi\pi^*(LE)$  at the  $S_0$  minimum. This ensures that the CI is energetically accessible after UV absorption.

Along reaction coordinate, we have noticed also an intersystem crossing (ISC) between  $^1\pi\pi^*(CT)$  singlet and  $^3\pi\pi^*(LE)$  triplet state at an O-H distance of about 1.08 Å, and is about 0.6 eV higher than the  $^3\pi\pi^*(LE)$  minimum. It is known that upon UV absorption, most of the population near the Franck-Condon region

reaches initially singlet excited states. The efficient population of the triplet manifold should take principally along the main decay process on singlet excited states. However, the singlet  $^1\pi\pi^*(LE)$  and the triplet  $^3\pi\pi^*(LE)$  states are located close in energy (about 0.45 eV) near the Franck-Condon region, which is an important element for obtaining significant vibrational overlap. After the  $^3\pi\pi^*(LE)$  electronic state is populated it reaches the  $^3\pi\pi^*(LE)$  equilibrium geometry located 0.74 eV below the  $^1\pi\pi^*(LE)$  minimum energy. These crossings of the  $^1\pi\pi^*(CT)$  with  $^1\pi\pi^*(LE)$ ,  $^3\pi\pi^*(LE)$  and  $S_0$  potential energy profiles show true conical intersections and intersystem crossing, which provide the mechanism of LE singlet and triplet states deactivation facilitating internal conversion to the ground state.

From Fig 4, we have noticed also that  $^1\pi\pi^*(CT)$  and  $^3\pi\pi^*(CT)$  states are degenerate since an O-H distance about 1.16 Å along the reaction path. Thus, the singlet excited state of PI form passes through the region of  $^1\pi\pi^*(CT)/^3\pi\pi^*(CT)$  degeneracy before decay to the ground state enhancing the probability of intersystem crossing.

This decay of nonradiative deactivation mechanism predicted here is in good agreement with previous experimental and theoretical studies applied to some relevant related molecular hydrogen bonding interactions where pyridine acts as a proton acceptor: 2-naphthylamine-pyridine <sup>1747</sup>, Dibenzocarbazole-pyridine <sup>1848,19</sup>, 1-aminopyrene-pyridine <sup>2020</sup>, 1-pyrenol-pyridine <sup>1747,21</sup>, indole-pyridine <sup>2424</sup>, pyrrole-pyridine <sup>2525,26,27</sup>, which provide the role of the  $^1\pi\pi^*(CT)$  state by connecting the  $^1\pi\pi^*(LE)$  state with the  $S_0$  state via conical intersections.

The same feature has been explained in previous works on the photophysical and photochemical properties of the cytosine-guanine <sup>4,5,6</sup> and adenine-thymine <sup>7,8</sup> DNA base pairs, proposed that after the excitation to the locally excited state  $^1\pi\pi^*(LE)$ , a conical intersection connecting the LE to a charge transfer excited state  $^1\pi\pi^*(CT)$  is readily accessible. Once in the CT state, the system evolves in a barrierless manner toward another CI crossing with the ground state  $S_0$ .

In similarly to the A' symmetry, the PI conformer of PhOH-Py complex with A'' symmetry constraint has been studied by constructing the RICC2/aug-cc-pVDZ PE profiles of ground and lowest singlet and triplet states along the O-H reaction coordinate (Fig. 5). The geometries of the lowest  $^1A''(\pi\sigma^*)$  singlet state have been optimized along the reaction path, while the energies of the electronic ground  $S_0$  and triplet  $^3A''(\pi\sigma^*)$  states were computed at the optimized geometry of the  $^1A''(\pi\sigma^*)$  state. The  $^1A''(\pi\sigma^*)$  state is dark, and it can be populated via a tunneling effect from the  $^1A'(\pi\pi^*(LE))$  state. This process is in competition with the quenching of the  $^1A'(\pi\pi^*(LE))$  state by the  $^1A'(\pi\pi^*(CT))$  state and to a lesser extent by the population of triplet states. Similarly, several studies of excited state dynamics of phenol and many substituted phenols predict that the excited state hydrogen transfer reaction occurs via H atom tunneling through the barrier generated by the  $^1\pi\pi^*-^1\pi\sigma^*$  conical intersection <sup>34,40</sup>.

As can be seen in Fig. 5, the stabilization of the dark  $^1A''(\pi\sigma^*)$  state is mediated by the H atom transfer from phenol to pyridine over a slightly repulsive PE profile to form the hydrogen transferred complex shown in Fig. 6(b1). This minimum is at an OH distance about 1.803 Å, with an energy of about 4.15 eV above the ground state minimum, is lower by about 0.4 eV and higher by 1.8 eV respectively than the minima of the  $^1A'(\pi\pi^*(LE))$  and  $^1A'(\pi\pi^*(CT))$  excited states. The conical intersection between the repulsive  $^1A''(\pi\sigma^*)$  state and the ground

Formatted

Formatted

Formatted

Formatted

Formatted

Formatted

state does not occur. The gap between these two states remains about 2.7 eV at the minimum of the  $^1A''(\pi\sigma^*)$  state. Moreover, Fig. 5 shows that  $^1A''(\pi\sigma^*)$  singlet and  $^3A''(\pi\sigma^*)$  triplet states are degenerate throughout the hydrogen migrating.

### 3.3.2. Pe conformer

In this section, potential energy profiles of the lowest excited states of Pe conformer of PhOH-Py complex are explored from the Franck-Condon to the conical intersection with the ground state  $S_0$ , at which the system can convert its excess electronic energy into vibrational energy and deactivate to the electronic ground state. In similarity to the Pl conformer, potential energy (PE) profiles as shown in Fig 7 and Fig 8 have been calculated along the minimum energy path (MEP) for an elongation of the O-H stretching coordinate in the Pe conformer of PhOH-Py complex at both  $A''$  and  $A'$  symmetries, for a given value of O-H, all remaining coordinates have been optimized for the lowest  $S_1$  excited state. The RICC2/aug-cc-pVDZ energies of the electronic ground  $S_0$  and triplet states were computed at the optimized geometry of the lowest  $S_1$  state.

Fig 7 shows the PE profiles of the ground  $S_0$ , the lowest singlet  $^1\pi\pi^*(CT1)$  and the lowest triplet  $^3\pi\pi^*(CT1)$  states of Pe conformer in  $A''$  symmetry. The adiabatic charge transfer  $^1A''(\pi\pi^*(CT1))$  and  $^3A''(\pi\pi^*(CT1))$  are predicted to be the lowest excited singlet and triplet states. Once the complex is excited to the  $^1\pi\pi^*(CT1)$  state in the Frank-Condon region, it quickly relaxes without barrier over a strongly repulsive potential energy profile to the minimum of the  $^1\pi\pi^*(CT1)$  where the system exhibits a bi-radical character electron/proton transferred complex, as indicated by its large dipole moment about 14 D. This hydrogen bonded  $PhO\cdots HPy$  bi-radical, shown in Fig. 6(b2), is lower in energy by about 1.63 eV than the locally excited triplet state  $^3\pi\pi^*(LE)$  minimum of PhOH-Py complex, and about 2.16 eV above the ground state minimum. Near the electron/proton transferred complex, one conical intersection  $^1A''(\pi\pi^*(CT1))/S_0$  exists and funnels the electron population to the  $S_0$  state, completing the internal conversion process. This crossing is at an O-H distance about 2.05 Å, and a corresponding energy about the same as the energy of the lowest  $^1\pi\pi^*(CT1)$  state of the electron/proton transferred complex.

In the potential energy function of  $A'$  symmetry, the minimum-energy approach was used to construct the PE profiles of the singlet excited states, where minimization of the  $^1\pi\pi^*(CT2)$  state energy was performed at each fixed value of the OH distance, while the energy of the ground and triplet states were calculated at the optimized geometry of the CT state. As it is shown in Fig. 8, the energies of the lowest excited states of the singlet  $^1\pi\pi^*(LE)$  and the triplet  $^3\pi\pi^*(LE)$  and of the ground state increase along the OH reaction coordinate. However, the PE profiles of the  $^1\pi\pi^*(CT2)$  and  $^3\pi\pi^*(CT2)$  excited states are essentially repulsive along the same reaction path. Fig. 8 shows that  $^1A'(\pi\pi^*(CT2))$  state can be populated over two intersections from  $^1A'(\pi\pi^*(LE))$  and to a lesser extent by  $^3A'(\pi\pi^*(LE))$  state. Thus, the PE of  $^1\pi\pi^*(CT2)$  crosses the  $^1\pi\pi^*(LE)$  and  $^3\pi\pi^*(LE)$  excited states at the OH distance of about 0.96 and 1.05 Å, respectively. The respective internal conversion and intersystem crossing points are about 5.1 eV and 4.4 eV above the ground state minimum for RICC2/aug-cc-pVDZ calculation, which provide the mechanism of LE singlet and triplet states deactivation. For OH distance of about 1.95 Å, the PE profile of  $^1A'(\pi\pi^*(CT2))$  state attend a minimum corresponding to the coupled electron/proton transferred complex (Fig. 6(a2)), which is about 1.35 eV higher than the same complex in the ground state. Therefore, for Pe conformer at  $A'$  symmetry, a secondary decay pathway for radiationless

relaxation to the ground state via  $^1\pi\pi^*(CT2)$ - $S_0$  conical intersection does not occur near this CT minimum, but it occurs at an O-H distance of about 3.5 Å

As in the case of PI conformer, Fig. 7 and Fig. 8 show that the  $^3A''(\pi\pi^*(CT1))$  triplet state is degenerate with the  $^1A''(\pi\pi^*(CT1))$  singlet state at almost any position of the migrating H atom. While, that  $^1A'(\pi\pi^*(CT2))$  and  $^3A'(\pi\pi^*(CT2))$  states are degenerate since an O-H distance about 1.2 Å along this reaction path.

### 3.3.3. Un conformer

The photophysics of electronically excited and ground states of the PhOH-Py complex without any symmetry constraint is connected to O-H bond. It consists of the lowest excited singlet, triplet and ground states potential energy exploration along O-H reaction coordinate and the decay at a region of excited and ground states degeneracy (near expected  $S_1/S_0$  conical intersection). The potential energy profiles for  $S_0$ , singlet and triplet states are shown in Fig 9. The geometries of the lowest  $^1\pi\pi^*(CT)$ , singlet state have been optimized along the reaction path, while the energies of the electronic ground  $S_0$  and excited singlet ( $^1\pi\pi^*(LE)$  and  $^1\pi\sigma^*$ ) and triplet ( $^3\pi\pi^*(LE)$  and  $^3\pi\pi^*(CT)$ ) states were calculated along the reaction path optimized in  $^1\pi\pi^*(CT)$  state. Here,  $^1\pi\pi^*(LE)$  and  $^1\pi\sigma^*$  states are higher in energy and does not play a role in the photophysics of the lowest excited states near the Franck-Condon region of the Un conformer, leading to nonradiative decay.

From Figure 9, we note that the Un conformer need not encounter the crossing between the  $^1\pi\pi^*(LE)$  and  $^1\pi\pi^*(CT)$  states in order to decay toward  $^1\pi\pi^*(CT)/S_0$  conical intersection. In other word, the decay is assigned to direct relaxation from the first  $^1\pi\pi^*(CT)$  state to the  $S_0$  state via conical intersection. The potential energy of the lowest  $^1\pi\pi^*(CT)$  state strongly decreases, in which the proton follows the electron and attaches to the N atom of pyridine leading to the formation of  $PhO\bullet\dots HPy\bullet$  bi-radical complex (Fig 6(c1)), which is equivalent to HAT from phenol to pyridine. For this complex, the ground and excited state are very close in energy ( $\Delta E = 0.066$  eV), thus a  $^1\pi\pi^*(CT)/S_0$  conical intersection is highly probable, which would induce a non-radiative decay to the  $S_0$  state. The  $^1\pi\pi^*(CT)$  is the lowest excited state along O-H reaction coordinate, which originates predominantly to  $LUMO+4 \leftarrow HOMO$  transition at 0.9 Å, changes to  $LUMO+2 \leftarrow HOMO$  at 1.0 Å, and since 1.2 Å, the transition becomes  $LUMO \leftarrow HOMO$ .

This system can also be compared with phenol-phenol dimer, where the nonradiative deactivation could be processed via direct  $^1\pi\pi^*/S_0$  conical intersection, but with a low barrier estimated to be about 0.4 eV, between the Franck-Condon point and this intersection <sup>3232</sup>

Formatted

## 3.4. Discussion

In the present study, we have applied RICC2 to explore the excited state deactivation pathways of PhOH-Py complex under  $C_s$  symmetry and without any symmetry constraints, by optimizing reaction pathways connecting different stationary structures. We saw that the major difference of the decay channels for different conformers is that the direct deactivation from  $^1\pi\pi^*(CT)$  to the ground state through the  $^1\pi\pi^*(CT)/S_0$  conical intersection for both Pe and Un conformers, while the PI conformer must encounter the region of  $^1\pi\pi^*(LE)/^1\pi\pi^*(CT)$  conical intersection, in which the wave function is a mixture of  $^1\pi\pi^*(LE)$  and  $^1\pi\pi^*(CT)$  character.

In this respect, the nonradiative decay could be qualified as an ultrafast for Pe and Un conformers, which is assigned to direct  ${}^1\pi\pi^*(CT) \rightarrow S_0$  deactivation, while a slower decay for Pl conformer, is assigned to indirect  ${}^1\pi\pi^*(CT) \rightarrow {}^1\pi\pi^*(LE) \rightarrow S_0$  deactivation.

Furthermore, it seems from our calculations that the radiationless relaxation to the ground state mediated by the coupled electron/proton transfer mechanism occurring on the A' surface is more favored in the Pl complex. Whereas, the same mechanism occurring on the A'' surface is more favored in the Pe complex. In addition, the  ${}^1A''(\pi\pi^*(CT1))/S_0$  conical intersection in Pe conformer was calculated to be lower by about 0.06 eV than that of  ${}^1A'(\pi\pi^*(CT))/S_0$  in Pl conformer.

The photophysics of isolated aromatic molecules in gas phase is usually a starting point and often a prerequisite toward understanding the photophysics when they are clustered with each other by intermolecular hydrogen bonding. In comparison with free phenol, the most notable effect of the complexation of phenol with pyridine is the removal of the conical intersection of the  ${}^1\pi\sigma^*$  state with the electronic ground state, which is replaced by the  ${}^1\pi\pi^*(CT)/S_0$  intersection. The RICC2/aug-cc-pVDZ potential energy profile of free phenol shows that the lowest singlet excited state A'( ${}^1\pi\pi^*$ ) is bound and its second excited state A''( ${}^1\pi\sigma^*$ ) is repulsive. The A''( ${}^1\pi\sigma^*$ ) state crosses A'( ${}^1\pi\pi^*$ ) at short O-H bond distance (about 1.13 Å) and then it reaches a nearly degenerate region with the ground state at large O-H bond distance, in which the energy difference goes from 0.1 eV at 2.1 Å to 0.07 eV at 2.2 Å (see Fig 10). Thus, the  ${}^1\pi\sigma^*/S_0$  conical intersection is highly probable, and then the hydrogen detachment from free phenol would induce a non-radiative decay to the ground state. This result is qualitatively supported by previous studies<sup>33,34,35,41</sup>. Here the energetic position of  ${}^1\pi\pi^*/{}^1\pi\sigma^*$  conical intersection cannot be exactly determined from Figure 10, because they are determined at different geometry optimizations (A' and A'' symmetries). However,  ${}^1\pi\sigma^*/S_0$  conical intersection is real, because the relevant PE profiles are determined at the same geometry optimization.

On the other hand, the free pyridine in the gas phase has been extensively studied experimentally as well as theoretically with regard to the photophysics and photochemistry of their low-lying excited singlet and triplet states<sup>42,43</sup>. It was found that both fluorescence from lowest  ${}^1n\pi^*$  singlet state and phosphorescence from low-lying triplet states are detected. Mataga et al<sup>44</sup> suggest that the formation of a complex between pyridine and electron-donating aromatics contributes to the quenching of pyridine triplet excited states. This suggestion is supported by our calculation, in which we have found that in the PhOH-Py complex the repulsive triplet CT state crosses the lowest triplet LE state through an accessible barrier, and then it becomes degenerate with the singlet excited state  ${}^1\pi\pi^*(CT)$  along reaction coordinate. Thus, the non-radiative decay of  ${}^3\pi\pi^*(CT)$  state has greater probability to occur after its intersystem crossing with the ground state.

In Figure 11 we compared for both Pl and Pe conformers, the RICC2/aug-cc-pVDZ behavior of the dipole moments of the lowest A' singlet state as a function of the O-H stretch coordinate with those obtained for A'' one. For Pl conformer, one can see that both A' and A'' states yield nearly similar steeply dipole moments increase with increasing O-H bond length as it is shown in Fig. 11 (a). The average dipole moment difference between these states is only about 0.4 D. This means that for both  ${}^1A'(\pi\pi^*)$  and  ${}^1A''(\pi\sigma^*)$  states and at the same OH bond length there are formation of complexes with the same charge distribution (bi-radical). The same situation is observed for the Pe conformer. Here, as it is shown in Fig 11 (b), the average dipole moment difference between A' and A'' states increases steeply with OH distance to about 1 D at  $d(O-H)=1.95$  Å. This

difference is related to the considerably NH out-of-plane formation on PhOH-Py complex in the case of  $^1A''(\pi\pi^*(CT1))$  state (see Fig. 6(b2)).

It should be also pointed out again that the CC2 method is very efficient to optimize excited states in the Franck-Condon region, but fails in the description of the conical intersection between the ground and the electronically excited state and between different excited states<sup>5</sup>. Multireference calculations (CASPT2 for example) with diffuse orbitals to take into account the Rydberg character of the  $\sigma^*$  orbital and with excited state optimization would be very useful to check more firmly our calculations.

#### 4. Conclusion

A comparative theoretical study of the nonradiative decay mechanisms of phenol-pyridine complex under Cs symmetry (PI and Pe conformers) and without symmetry constraints has been performed by the RICC2 calculation method with the use of aug-cc-pVDZ basis set. In particular, the RIMP2 coupled with RICC2 method have been employed even for geometry optimization in the ground and excited states and reaction paths relevant to the deactivation process. In our study, we have discussed also situations where the triplet states are populated and may contribute to the excited state photophysics.

The decay mechanism of the nonradiative deactivation process in PhOH-Py complex for PI, Pe (at  $A'$  and  $A''$  symmetries) and unconstrained conformers, is connected to the O-H bond dissociation and the  $S_1/S_0$  conical intersection. The reaction along O-H bond, mediated by a coupled electron/proton transfer in PI, Pe and Un conformers, leads to deactivation, respectively over  $^1A'(\pi\pi^*(CT))-S_0$ ,  $^1A''(\pi\pi^*(CT))-S_0$  and  $^1\pi\pi^*(CT)-S_0$  conical intersections. For PI conformer, the conical intersections founded are lower than the local minima of excited singlet and triplet states. This decay of radiationless relaxation to the ground state, is rationalized in terms of conical intersections and singlet-triplet ISC connecting the different states, where, several possible pathways are in competition. In this respect, two readily accessible conical intersections  $^1A'(\pi\pi^*(LE))/^1A'(\pi\pi^*(CT))$  and  $^1A'(\pi\pi^*(CT))/S_0$  in the gas phase, encountered along the reaction path are responsible for the fluorescence quenching. Whereas for Pe and Un conformers, the nonradioactive decay is assigned to direct relaxation from the  $^1A''(\pi\pi^*(CT))$  and  $^1\pi\pi^*(CT)$  states, respectively to the ground state via conical intersection. Furthermore, we have brought up to light, for the first time, for these hydrogen bonding interactions, the phosphorescence quenching proceeds via triplet-singlet ( $^3\pi\pi^*(LE)-^1\pi\pi^*(CT)$ ) and triplet-triplet ( $^3\pi\pi^*(LE)-^3\pi\pi^*(CT)$ ) crossings, followed by ( $^3\pi\pi^*(CT)-^1\pi\pi^*(CT)$ ) degeneracy. These findings imply that the  $\pi\pi^*(CT)$  acts as a doorway state in the nonradiative excited states.

Finally, for these categories of hydrogen bonding interactions the photodissociation of the bi-radical is a less probable process since there are successive internal conversions to the ground state along reaction coordinate, which are insured by the conical intersection between the lowest excited and ground states.

#### Acknowledgments

The authors are grateful to Professor Christophe Juvet (University of Aix-Marseille) for his valuable comments and helpful discussions.

## References

- 1 Hydrogen Bonding and Transfer in the Excited State, ed. K. -L. Han and G. -J. Zhao, Wiley, West Sussex, UK, 2011.
- 2 G. J. Zhao and K. L. Han, *J. Phys. Chem A.*, 2007, **111**, 2469-2474
- 3 G. J. Zhao and K. L. Han, *Acc. Chem. Res.*, 2012, **45**, 404.
- 4 A. L. Sobolewski and W. Domcke, *Phys. Chem. Chem. Phys.*, 2004, **6**, 2763-2771.
- 5 A. L. Sobolewski, W. Domcke and C. Hattig, *Proc. Natl. Acad. Sci. U.S.A.*, 2005, **102**, 17903-17906.
- 6 S. Yamazaki and T. Taketsugu, *Phys. Chem. Chem. Phys.*, 2012, **14**, 8866-8877.
- 7 S. Perun, A. L. Sobolewski and W. Domcke, *J. Phys. Chem A.*, 2006, **110**, 9031-9038.
- 8 J. P. Gobbo, V. Saurí, D. Roca-Sanjuán, L. Serrano-Andrés, M. Merchán and A. C. Borin., *J. Phys. Chem. B.*, 2012, **116**, 4089-4097.
- 9 G. Groenhof, M. Boggio-Pasqua, M. Goette, H. Grubmüller and M.A. Robb, *J. Am. Chem. Soc.*, 2007, **129**, 6812–6819.
- 10 P.R.L. Markwick and N.L. Doltsinis., *J. Chem. Phys.*, 2007, **126**, 175102
- 11 M. Barbatti, A.J.A. Aquino, J.J. Szymczak, D. Nachtigallová, P. Hobza and H. Lischka, *Proc. Nat. Acad. Sci. USA.*, 2010, **107**, 21453
- 12 C.E. Crespo-Hernandez, B. Cohen, J. Hare and B. Kohler, *Chem. Rev.*, 2004, **104**, 1977.
- 13 T. Förster, *Elektrochem.*, 1950, **54**, 531.
- 14 L. G. Arnaut and S. J. Formosinho, *J. Photochem. Photobiol. A.*, 1993, **75**, 1.
- 15 H. Tanaka and K. Nishimoto, *J. Phys. Chem.* 1984, **88**, 1052.
- 16 N. Mataga, *Pure Appl. Chem.*, 1984, **56**, 1255.
- 17 N. Ideka, T. Okada and N. Mataga, *Chem. Phys. Lett.*, 1980, **69**, 251.
- 18 M. M. Martin, N. Ideka, T. Okada and N. Mataga, *J. Phys. Chem.*, 1982, **86**, 4148.
- 19 M. M. Martin, H. Miyasaka, A. Karen and N. Mataga, *J. Phys. Chem.*, 1985, **89**, 182-185.
- 20 N. Ideka, H. Miyasaka, T. Okada, and N. Mataga, *J. Am. Chem. Soc.*, 1983, **105**, 5206-5211.
- 21 H. Miyasaka, A. Tabata, S. Ojima, N. Ideka and N. Mataga, *J. Phys. Chem.*, 1993, **97**, 8222.
- 22 N. Mataga and H. Miyasaka, *Adv. Chem. Phys.* 1999, **107**, 431-496.
- 23 J. Waluk, *Acc. Chem. Res.*, 2003, **36**, 832.
- 24 A. L. Sobolewski and W. Domcke, *J. Phys. Chem. A.*, 2007, **111**, 11725.
- 25 M. F. Rode and A. L. Sobolewski, *Chem. Phys.*, 2008, **347**, 413.
- 26 L. M. Frutos, A. Markmann, A. L. Sobolewski and W. Domcke, *J. Phys. Chem. B.*, 2007, **111**, 6110.
- 27 Z. Lan, L.M. Frutos, A.L. Sobolewski and W. Domcke, *Proc. Nat. Acad. Sci USA.*, 2008, **105**, 12707-12712.
- 28 R. Ahlrichs, M. Bär, M. Häser, H. Horn and C. Kölmel, *Chem. Phys. Lett.*, 1989, **162**, 165.
- 29 F. Weigend, M. Haser, H. Patzelt and R. Ahlrichs, *Chem. Phys. Lett.*, 1998, **294**, 143.
- 30 C. Hätig, *J. Chem. Phys.*, 2003, **118**, 7751.
- 31 A. Köhn and C. Hätig, *J. Chem. Phys.*, 2003, **119**, 5021.
- 32 V. Poterya, L. Šišťík, P. Slavíček and M. Fárník, *Phys. Chem. Chem. Phys.*, 2012, **14**, 8936.
- 33 Z. Lan, W. Domcke, V. Vallet, A. L. Sobolewski and S. Mahapatra, *J. Chem. Phys.*, 2005, **122**, 224315.
- 34 R. N. Dixon, T. A. A. Oliver and M. N. R. Ashfold, *J. Chem. Phys.*, 2011, **134**, 194303.

- 
- 35 A. L. Sobolewski and W. Domcke, *J. Phys. Chem. A.*, 2001, **105**, 9275.
- 36 K. Daigoku, S. Ishiuchi, M. Sakai, M. Fujii and K. Hashimoto, *J. Chem. Phys.*, 2003, **119**, 5149.
- 37 M. Merchán, L. Serrano-Andrés, M.A. Robb and L. Blancafort L, *J. Am. Chem. Soc.*, 2005, **127**, 1820-1825.
- 38 T. Climent, R. González-Luque, M. Merchán and L. Serrano-Andrés, *Chem. Phys. Lett.*, 2007, **441**, 327-331.
- 39 J.J. Serrano-Pérez, R. González-Luque, M. Merchán and L. Serrano-Andrés, *J. Phys. Chem. B.*, 2007, **111**, 11880-11883.
- 40 G. A. Pino, A. N. Oldani, E. Marceca, M. Fujii, S. I. Ishiuchi, M. Miyazaki, M. Broquier, C. Dedonder and C. Juvet, *J. Chem. Phys.*, 2010, **133**, 124313.
- 41 A. L. Sobolewski, W. Domcke, C. D. Lardeux and C. Juvet, *Phys. Chem. Chem. Phys.*, 2002, **4**, 1093.
- 42 M. Chachivilis and A. H. Zewail, *J. Phys. Chem A.*, 1999, **103**, 7408-7418.
- 43 Z. L. Cai and J. R. Reimers, *J. Phys. Chem A.*, 2000, **104**, 8389-8408.
- 44 V. Hirata and N. Mataga, *J. Phys. Chem.*, 1984, **88**, 3091.

**Table 1:** Relative stabilities (eV), vertical singlet excitation energies, Dipole moment  $\mu$ (D) and oscillator strength  $f$  of the lowest singlet excited states computed at the RICC2 level for P1 and Pe conformers of PhOH-Py under Cs symmetry.  $S_0$  RICC2 is the RICC2 ground state energy computed at the corresponding RIMP2 optimized geometry

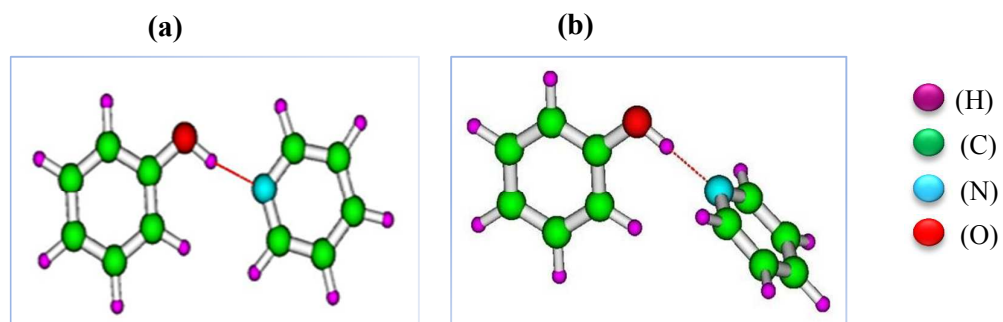
	P1 conformer				Pe conformer			
	E	Transition	$\mu$	$f$	E	Transition	$\mu$	$f$
<b><math>S_0</math> RIMP2</b>	0	-	5.22	-	-0.02	-	5.47	-
<b><math>S_0</math> RICC2</b>	0	-	5.22	-	-0.02	-	5.47	-
<b>1 <math>^1A'</math></b>	4.74	$\pi\pi^*(LE)$ (60%)	5.93	0.034	4.73	$\pi\pi^*(LE)$ (43%)	5.47	0.038
<b>2 <math>^1A'</math></b>	5.20	$\pi\pi^*(Py)$ (48%)	1.12	0.029	5.20	$n\sigma^*$ (51%)	0.82	0.007
<b>3 <math>^1A'</math></b>	5.26	$\pi\pi^*(CT)$ (64%)	13.38	0.011	5.55	$\pi\pi^*(CT)$ (67%)	12.88	0.004
<b>1 <math>^1A''</math></b>	5.17	$\pi\sigma^*$ (38%)	7.21	$8.10^{-4}$	5.02	$\pi\pi^*(CT)$ (43%)	12.89	$6.10^{-4}$
<b>2 <math>^1A''</math></b>	5.62	$\pi\sigma^*$ (32%)	6.72	0.001	5.17	$\pi\sigma^*$ (40%)	1.96	$10^{-5}$
<b>3 <math>^1A''</math></b>	5.67	$\pi\sigma^*$ (25%)	2.94	0.004	5.21	$\pi\pi^*(Py)$ (39%)	4.37	0.034

**Table 2:** Relative energies E(eV), Dipole moment  $\mu$ (D) and oscillator strength f of the lowest singlet excited states computed with the RICC2/aug-cc-pVDZ level at the  $S_1$  minimum of PI conformer in  $A'$  symmetry. Optimization of Pe conformer with aug-cc-pVDZ basis does not converged.

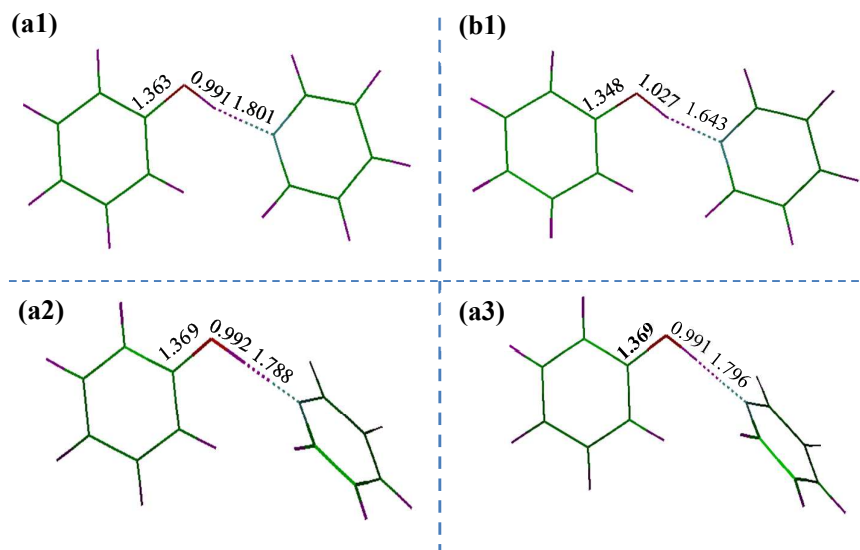
State	PI conformer			
	E(eV)	Transition	$\mu$	f
<b>1</b> $^1A'$	4.53	$\pi\pi^*(LE)$ (62%)	6.39	0.042
<b>2</b> $^1A'$	4.89	$\pi\pi^*(CT)$ (84%)	16.68	0.016
<b>3</b> $^1A'$	5.37	$\pi\pi^*$ (Py) (42%)	1.62	0.022
<b>1</b> $^1A''$	5.08	$\pi\sigma^*$ (36%)	7.06	$3.0 \cdot 10^{-4}$
<b>2</b> $^1A''$	5.5	$\pi\sigma^*$ (33%)	7.45	$1.7 \cdot 10^{-3}$
<b>3</b> $^1A''$	5.55	$\pi\sigma^*$ (26%)	3.65	$2.5 \cdot 10^{-3}$

**Table 3:** Relative energies E(eV), Dipole moment  $\mu$ (D) of the lowest triplet excited states computed at the RICC2 level with the aug-cc-pVDZ basis set for both Pl and Pe conformer in Cs symmetry.

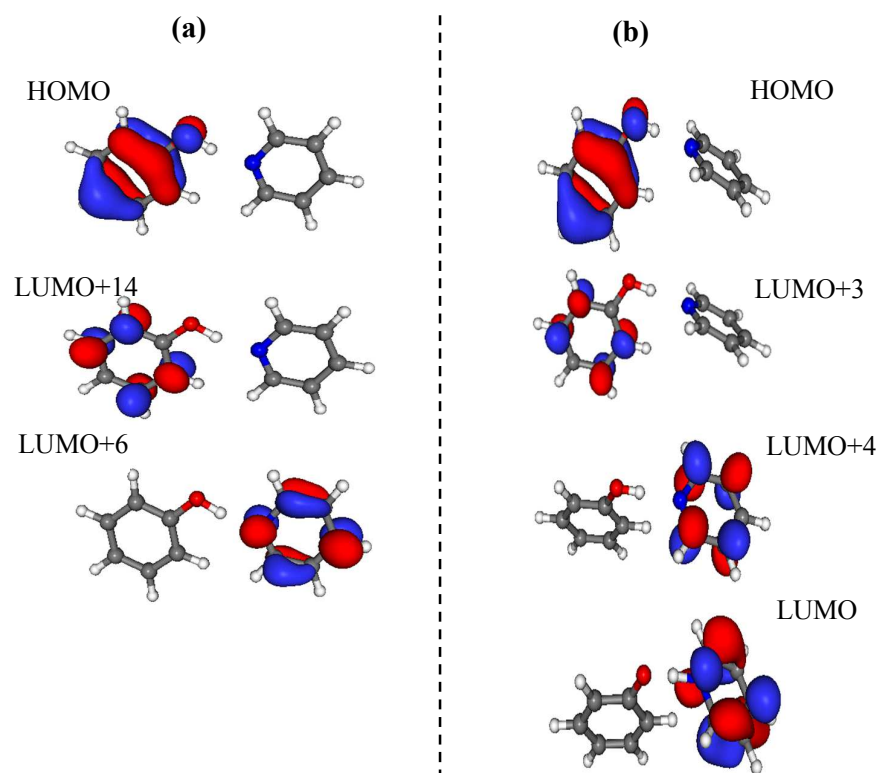
State	Pl conformer			Pe conformer		
	E(eV)	Transition	$\mu$	E(eV)	Transition	$\mu$
<b>1</b> <sup>3</sup> A'	3.79	$\pi\pi^*$ (LE) (71%)	5.93	3.79	$\pi\pi^*$ (LE) (65%)	5.61
<b>2</b> <sup>3</sup> A'	4.81	$\pi\pi^*$ (LE) (23%)	5.84	4.82	$\pi\pi^*$ (CT) (20%)	5.84
<b>3</b> <sup>3</sup> A'	4.82	$\pi\pi^*$ (Py) (30%)	6.11	4.83	$\pi\pi^*$ (Py) (45%)	5.63
<b>1</b> <sup>3</sup> A''	5.3	$\pi\sigma^*$ (36%)	7.19	5.06	$\pi\pi^*$ (CT) (29%)	14.36
<b>2</b> <sup>3</sup> A''	5.74	$\pi\sigma^*$ (39%)	6.41	5.24	$\pi\pi^*$ (Py) (34%)	5.47
<b>3</b> <sup>3</sup> A''	5.78	$\pi\sigma^*$ (28%)	2.25	5.31	$\pi\sigma^*$ (39%)	3.04



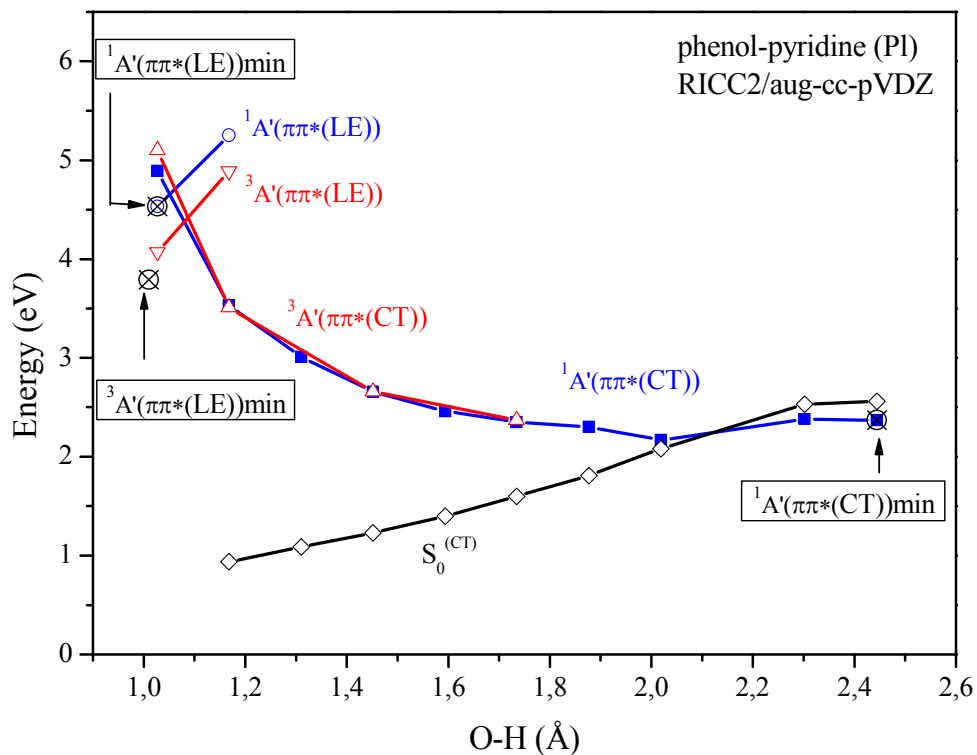
**Figure 1.** Phenol-Pyridine complex. (a) planar (Pl) conformer, (b) perpendicular (Pe) conformer.



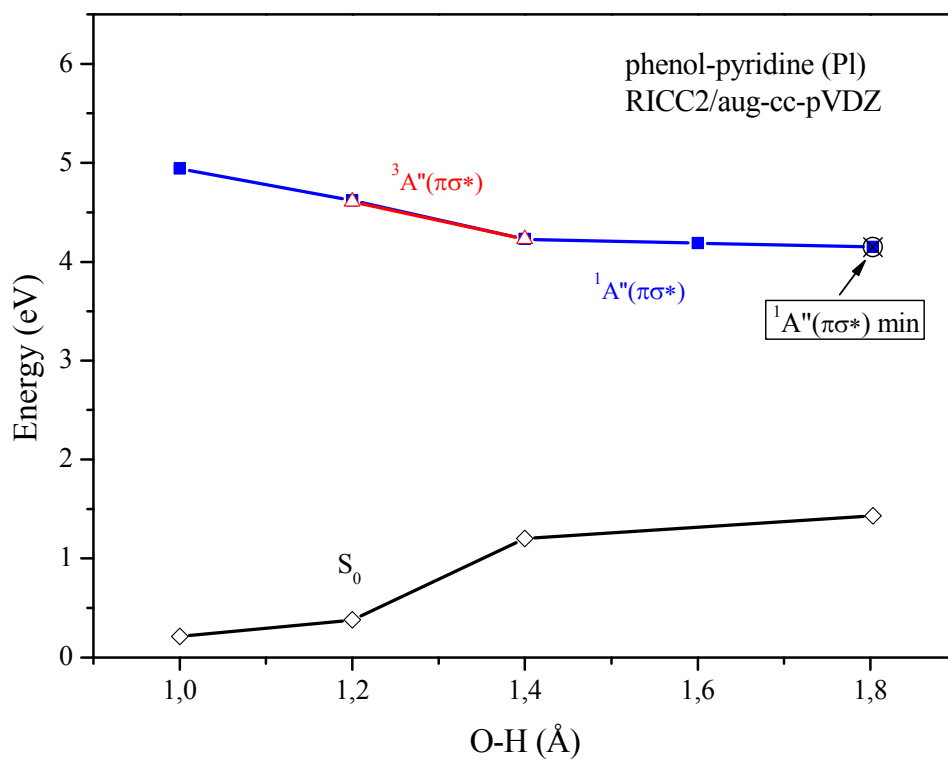
**Figure 2.** RICC2/aug-cc-pVDZ optimized structures of PhOH-Py complex under Cs symmetry (PI and Pe conformers) ((a1) and (a2)) and without symmetry constraints (a3) in their ground state. (b1) represents the minimum lowest excited state of PI conformer.



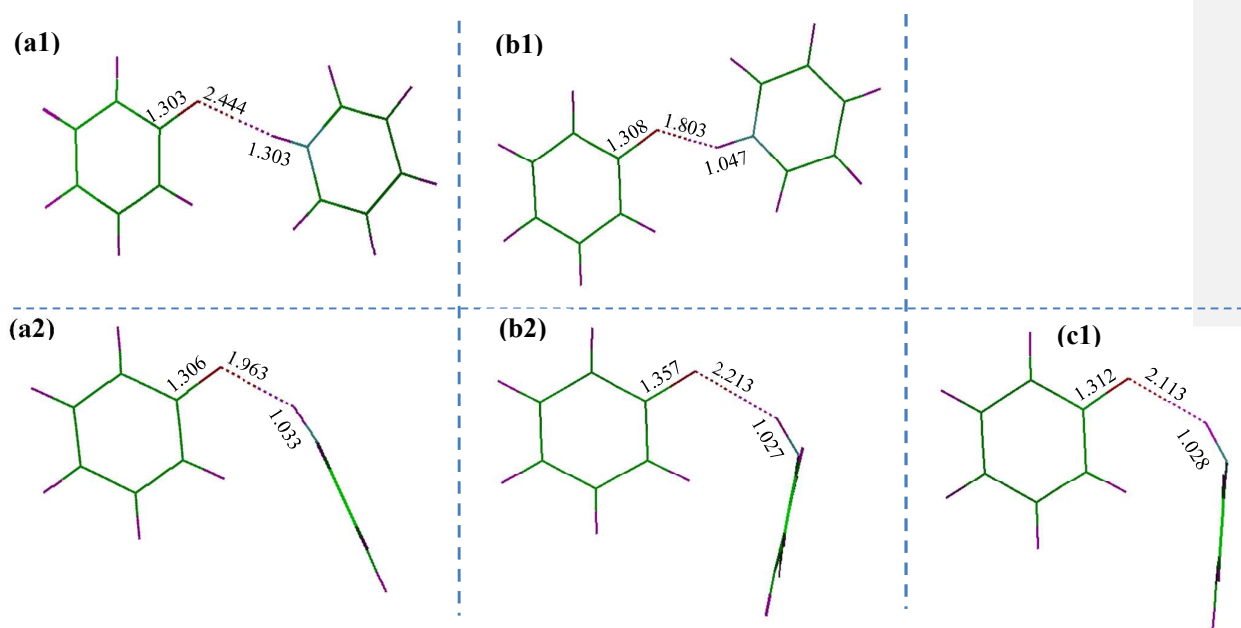
**Figure 3.** Molecular orbitals which are involved in electron transitions in PI (a) and Pe (b) conformers of PhOH-Py complex.



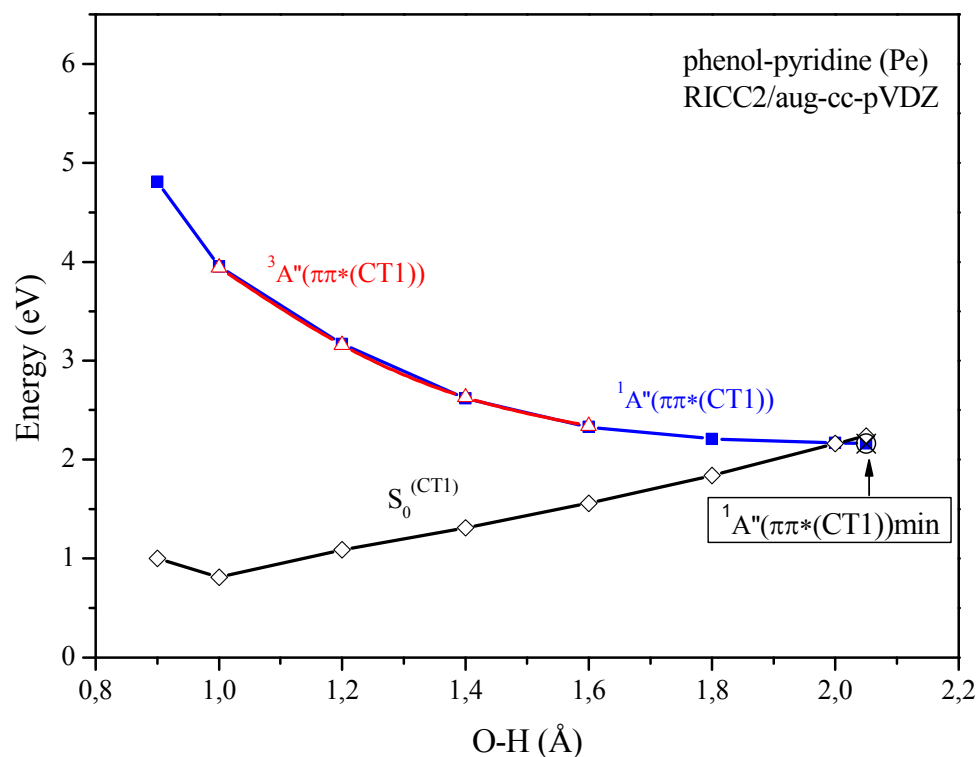
**Figure 4.** Potential energy profiles of the electronic ground state  $S_0$  ( $\diamond$ ), the lowest singlet  $^1\pi\pi^*(LE)$  ( $\circ$ ) and  $^1\pi\pi^*(CT)$  ( $\blacksquare$ ), and the lowest triplet  $^3\pi\pi^*(LE)$  ( $\nabla$ ) and  $^3\pi\pi^*(CT)$  ( $\triangle$ ) excited states of the PI conformer for phenol-pyridine complex, calculated at the RICC2/aug-cc-pVDZ level as function of the proton transfer coordinate (O-H) with  $A'$  symmetry constraint. The energies of the ground and triplet states have been calculated at the optimized geometries of the  $^1\pi\pi^*(CT)$  (or  $^1\pi\pi^*(LE)$ ) state. ( $\otimes$ ) symbols represent minimum energies of the lowest singlet and triplet excited states of PhOH...Py complex and its corresponding electron/proton transferred complex PhO...HPy. The RICC2 ground state energy computed at the corresponding RIMP2 optimized geometry is used as the energy reference.



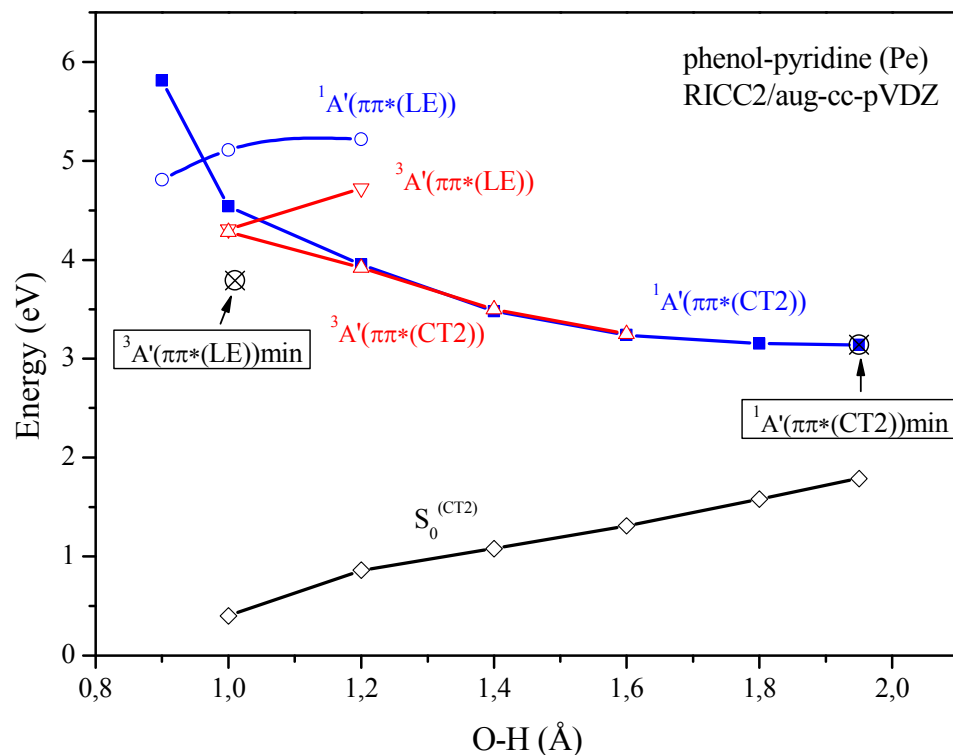
**Figure 5.** Potential energy profiles of the ground state  $S_0$  ( $\diamond$ ), the lowest singlet  $^1\pi\sigma^*$  ( $\blacksquare$ ), and triplet  $^3\pi\sigma^*$  ( $\triangle$ ) excited states of the PI conformer for phenol-pyridine complex, calculated at the RICC2/aug-cc-pVDZ level as function of the hydrogen transfer coordinate (O-H) with  $A''$  symmetry constraint. The energies of the ground and triplet states have been calculated at the optimized geometries of the  $^1\pi\sigma^*$  state. ( $\otimes$ ) symbol represents minimum energy of the lowest singlet  $^1\pi\sigma^*$  excited state of the hydrogen transferred complex  $\text{PhO}\cdot\cdots\text{HPy}\cdot$ . The RICC2 ground state energy computed at the corresponding RIMP2 optimized geometry is used as the energy reference.



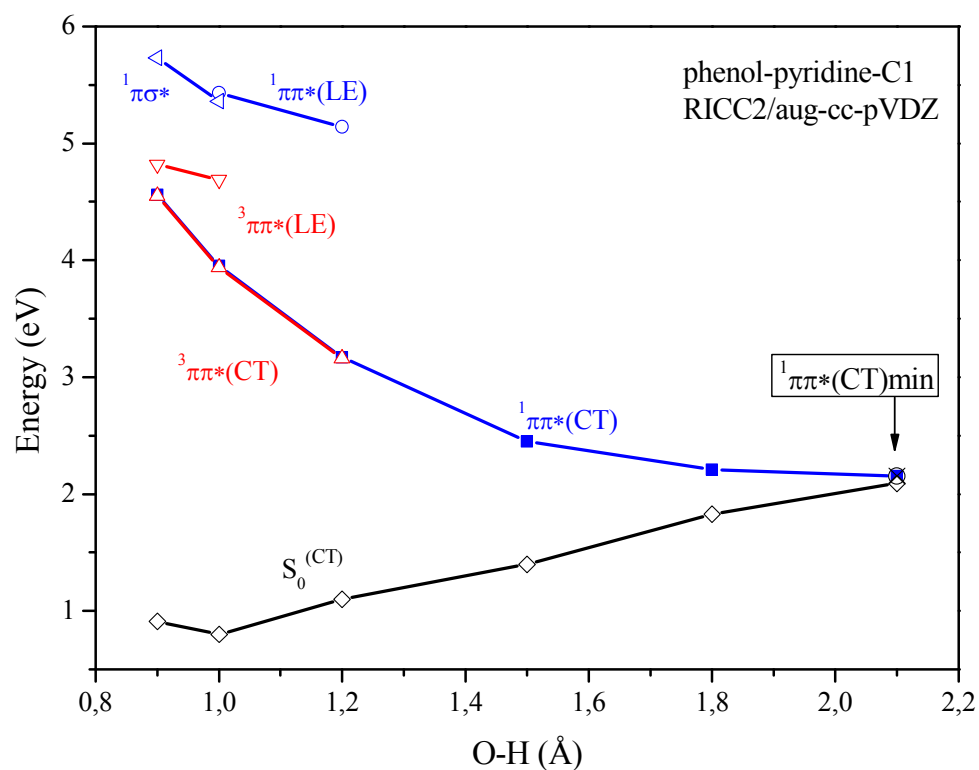
**Figure 6.** Optimized structures of hydrogen bonded PhO•...HPy• bi-radical in their lowest singlet excited  $^1A'$  ((a1) and (a2)) and  $^1A''$  ((b1) and (b2)) excited states of PI and Pe conformers ( $C_s$  symmetry) and unconstrained geometry (c1)



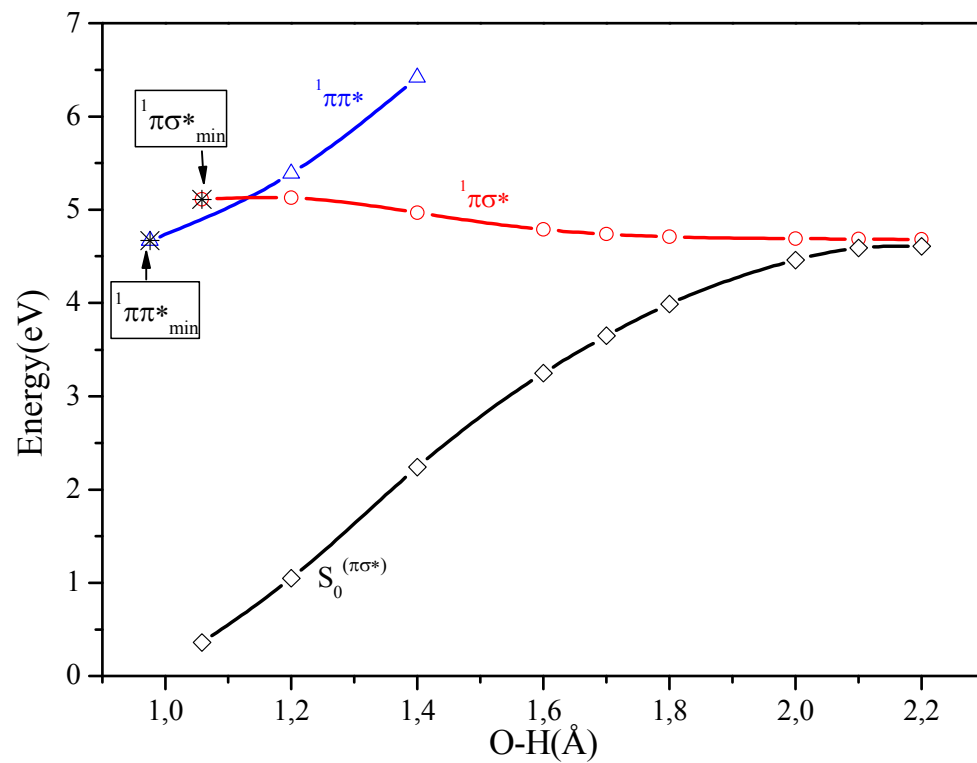
**Figure 7.** Potential energy profiles of the ground state  $S_0$  ( $\diamond$ ), the lowest singlet  $\pi\pi^*(CT1)$  ( $\blacksquare$ ), and triplet  $^3\pi\pi^*(CT1)$  ( $\triangle$ ) excited states of the Pe conformer for phenol-pyridine complex, calculated at the RICC2/aug-cc-pVDZ level as function of the proton transfer coordinate (O-H) with  $A''$  symmetry constraint. The energies of the ground and triplet states have been calculated at the optimized geometries of the  $^1\pi\pi^*(CT1)$  state. ( $\otimes$ ) symbol represents minimum energy of the lowest singlet  $\pi\pi^*(CT1)$  excited state of the electron/proton transferred complex  $\text{PhO}\cdots\text{HPy}$ . The RICC2 ground state energy computed at the corresponding RIMP2 optimized geometry is used as the energy reference.



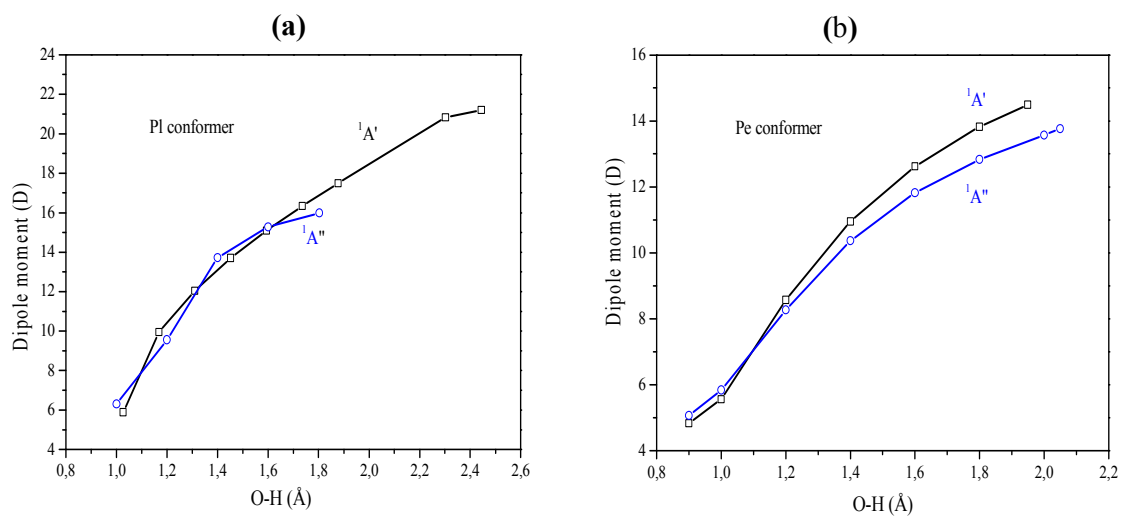
**Figure 8.** Potential energy profiles of the electronic ground state  $S_0$  ( $\diamond$ ), the lowest singlet  $^1\pi\pi^*(LE)$  ( $\circ$ ) and  $^1\pi\pi^*(CT2)$  ( $\blacksquare$ ), and the lowest triplet  $^3\pi\pi^*(LE)$  ( $\nabla$ ) and  $^3\pi\pi^*(CT2)$  ( $\triangle$ ) excited states of the Pe conformer for phenol-pyridine complex, calculated at the RICC2/aug-cc-pVDZ level as function of the proton transfer coordinate (O-H) with  $A'$  symmetry constraint. The energies of the ground and triplet states have been calculated at the optimized geometries of the  $^1\pi\pi^*(CT2)$  state. ( $\otimes$ ) symbols represent minimum energies of the lowest singlet and triplet excited states of PhOH...Py complex and its corresponding electron/proton transferred complex PhO...HPy. The RICC2 ground state energy computed at the corresponding RIMP2 optimized geometry is used as the energy reference.



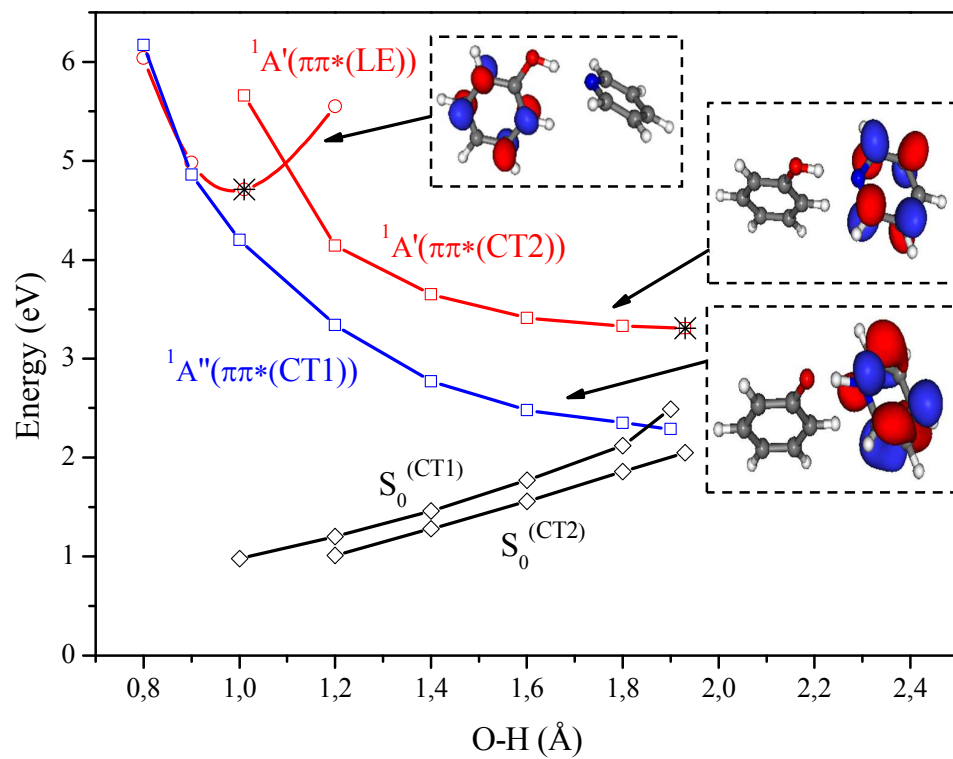
**Figure 9.** Potential energy profiles of the electronic ground state  $S_0$  ( $\diamond$ ), the lowest singlet  $^1\pi\pi^*(LE)$  ( $\circ$ ) and  $^1\pi\pi^*(CT)$  ( $\blacksquare$ ), and the lowest triplet  $^3\pi\pi^*(LE)$  ( $\nabla$ ) and  $^3\pi\pi^*(CT)$  ( $\triangle$ ) excited states of the phenol-pyridine complex without symmetry constraints. The energies of the ground and triplet states have been calculated at the optimized geometries of the  $^1\pi\pi^*(CT)$  state. ( $\otimes$ ) symbol represents minimum energies of the lowest excited coupled electron/proton transferred complex  $\text{PhO}\cdot\cdots\text{HPy}\cdot$ . The RICC2 ground state energy computed at the corresponding RIMP2 optimized geometry is used as the energy reference.



**Figure 10.** Potential energy profiles of the electronic ground state  $S_0$  ( $\diamond$ ), the lowest singlet excited states  ${}^1\pi\pi^*$  ( $\Delta$ ) and  ${}^1\pi\sigma^*$  ( $\circ$ ) of phenol along hydrogen detachment.



**Figure 11.** RICC2/aug-cc-pVDZ dipole moments of the lowest singlet  $^1A'$  ( $\square$ ), and  $^1A''$  ( $\circ$ ) excited states for both PI (a) and Pe (b) conformers of the phenol-pyridine complex, as a function of the O-H stretch reaction coordinate.



Graphical abstract